

Spectral function of electron-phonon models by cluster perturbation theory

Martin Hohenadler, Markus Aichhorn, and Wolfgang von der Linden

*Institute for Theoretical Physics, Graz University of Technology, Petersgasse 16, A-8010 Graz, Austria**

Cluster perturbation theory in combination with the Lanczos method is used to compute the one-electron spectral function of the Holstein polaron in one and two dimensions. It is shown that the method allows reliable calculations using relatively small clusters, and at the same time significantly reduces finite-size effects. Results are compared with exact data and the relation to existing work is discussed. We also use a strong-coupling perturbation theory—equivalent to the Hubbard I approximation—to calculate the spectral function of the quarter-filled Holstein model of spinless fermions, starting from the exact atomic-limit Green function. The results agree well with previous calculations within the many-body coherent potential approximation.

PACS numbers: 63.20.Kr 71.27.+a 71.38.-k

I. INTRODUCTION

Spectral properties, such as the one-electron spectral function, provide valuable insight into the usually complex physics of strongly correlated systems. However, reliable results for such quantities are difficult to obtain. Analytical methods are often restricted to very simple limiting cases, and results can usually not be extended to more general situations. Two remarkable exceptions are the Holstein model with linear electron dispersion^{1,2} and the Hubbard model,³ both in one dimension, which have been solved exactly. To study more general models, numerical methods such as Exact Diagonalization (ED) and Quantum Monte Carlo (QMC) have received much attention over the last decades. ED methods allow very accurate calculations of ground-state as well as finite-temperature spectral properties, but are restricted to rather small clusters due to the large dimension of the corresponding Hilbert space. QMC can be used to obtain results on large clusters even in higher dimensions, but here the sign-problem and the ill-posed analytic continuation required to obtain dynamic correlation functions for real frequencies are detrimental for many interesting applications.

The recently developed cluster perturbation theory^{4,5} (CPT) marks an important improvement of the situation. It is based on a break-up of the infinite system into identical, finite clusters, on which the one-electron Green function is calculated exactly. Then, the hopping between clusters is treated within strong-coupling perturbation theory^{6,7} (SCPT). The method has been successfully used for various Hubbard models, to calculate spectral functions, as well as other quantities of interest, both for zero^{4,5,8} and finite temperature.⁹ Although the concept of CPT relies on a model with local interactions only, it has also been applied with some success to the $t - J$ model.^{10,11} For the calculation of the cluster Green function, the ED Lanczos method (for a review see Ref. 12) can be used.

For the case of coupled electron-phonon systems, such as the Holstein model and its various extensions—e.g. the Holstein-Hubbard or the Holstein double-exchange

model—the application of ED methods is hampered by the infinite number of possible phonon configurations, which gives rise to a rapidly growing requirement of computer memory and/or CPU time as the number of lattice sites or phonon states increases. Consequently, standard ED methods—employing some kind of Hilbert space truncation—are restricted to very small clusters, especially for low phonon frequency and/or strong electron-phonon coupling. Again improved methods such as DMRG, or the use of variational phonon bases allow to extend the accessible parameter range. Nevertheless, as electron-phonon interaction has been identified as an important ingredient in, e.g., high-temperature superconductors¹³ and manganites¹⁴, further progress along these lines is highly desirable.

In this paper, we show that CPT can be successfully applied to electron-phonon models with a (local) coupling of the Holstein type.¹⁵ We present results for the one-electron spectral function of the Holstein polaron, i.e. the Holstein model with one electron, in one and two dimensions. The Holstein polaron problem has been investigated intensively in the past, and a wealth of information about its spectral properties is available. We find that the use of CPT strongly reduces finite-size effects, giving results which are much closer to the thermodynamic limit than the corresponding ED data. Additionally, we consider the special case of a completely saturated ferromagnetic state at zero temperature in the Holstein double-exchange model¹⁶ for colossal magnetoresistive manganites. The latter is then equivalent to the Holstein model of spinless fermions, and we combine the exact atomic-limit one-particle Green function with CPT for a single-site cluster to calculate the spectral function at quarter-filling. The results of this simple approach agree well with the previously developed many-body coherent potential approximation.^{14,16,17,18,19}

The paper is organized as follows: In Sec. II we give a review of CPT. Sec. III discusses the application to the Holstein polaron, while the SCPT for the many-electron case is presented in Sec. IV. Finally, Sec. V contains our conclusions.

II. CLUSTER PERTURBATION THEORY

The basic idea of CPT^{4,5} is to divide the infinite lattice into identical clusters, each containing N lattice sites. Adopting the notation of Ref. 5, the Hamiltonian of the system is written in the form $H = H_0 + V$ where

$$H_0 = \sum_{\mathbf{R}} H_0^{\mathbf{R}}, \quad V = \sum_{\substack{\mathbf{R}, \mathbf{R}' \\ a, b}} V_{a,b}^{\mathbf{R}, \mathbf{R}'} c_{\mathbf{R}a}^\dagger c_{\mathbf{R}'b}. \quad (1)$$

In the most general formulation of CPT,⁵ the subscripts a, b denote different orbitals within a cluster, but here we restrict ourselves to the case of one orbital per site so that $a, b = 1, \dots, N$. The vectors \mathbf{R}, \mathbf{R}' correspond to sites in the superlattice of clusters (see Ref. 5). In Eq. (1), $H_0^{\mathbf{R}}$ represents a Hamiltonian of a single cluster—containing local interactions only—and V describes the hopping between clusters, i.e. the hopping amplitude between site a of cluster \mathbf{R} and site b of cluster \mathbf{R}' is given by the matrix element $V_{a,b}^{\mathbf{R}, \mathbf{R}'}$. Although long-range hopping can also be included,⁵ we shall only consider models with nearest-neighbor hopping so that $V_{a,b}^{\mathbf{R}, \mathbf{R}'} = -t$ for neighboring sites a, b in adjacent clusters \mathbf{R}, \mathbf{R}' . Within CPT, an approximation for the Green function of the original system, $\mathcal{G}(\mathbf{k}, \epsilon)$, is obtained using an analytical strong-coupling perturbation expansion up to first order of the inter-cluster hopping V (for details of the derivation see Ref. 5). The resulting equation relating the Green function of the original lattice to the energy-dependent cluster Green function $G(z)$ reads^{4,5}

$$\mathcal{G}_{ab}(\mathbf{Q}, z) = \left(\frac{G(z)}{1 - V(\mathbf{Q})G(z)} \right)_{a,b}. \quad (2)$$

Here $z = \epsilon + i\eta$, $G(z)$ and $V(\mathbf{Q})$ stand for $N \times N$ matrices, and the inter-cluster hopping V has been partially Fourier-transformed exploiting the translational symmetry of the cluster superlattice, with \mathbf{Q} being a wave vector of the reduced Brillouin zone.⁵ Finally, the Green function \mathcal{G}_{ab} can be transformed from the mixed representation of Eq. (2), real space within a cluster and reciprocal space between clusters, using⁵

$$\mathcal{G}(\mathbf{k}, z) = \frac{1}{N} \sum_{a,b=1}^N \mathcal{G}_{ab}(\mathbf{k}, z) e^{-i\mathbf{k} \cdot (\mathbf{r}_a - \mathbf{r}_b)} \quad (3)$$

to obtain the familiar representation of the one-electron Green function. $\mathcal{G}(\mathbf{k}, z)$ as given by Eqs. (2) and (3) becomes exact in the atomic limit $t = 0$ (Refs. 4,5). Moreover, it also reduces to the exact result for the case of non-interacting electrons^{4,5} since, in this case, Eq. (2) corresponds to the exact resummation of the perturbation series. Finally, CPT also becomes exact in the limit $N \rightarrow \infty$ (Refs. 4,5). The one-electron cluster Green func-

tion at zero temperature

$$G_{ab}(\epsilon) = \langle \Omega | c_a \frac{1}{z - (H_0 - E_0)} c_b^\dagger | \Omega \rangle + \langle \Omega | c_b^\dagger \frac{1}{z + (H_0 - E_0)} c_a | \Omega \rangle \quad (4)$$

can be calculated exactly for any pair of site indices a, b in the cluster using, e.g., the Lanczos method. Here E_0 is the energy of the ground state $|\Omega\rangle$ of the cluster, and a spin index has been suppressed in the notation. The two parts of the Green function matrix G_{ab} correspond to adding or removing an electron to/from $|\Omega\rangle$. Finally, the one-electron spectral function is defined as

$$A(\mathbf{k}, \epsilon) = -\pi^{-1} \lim_{\eta \rightarrow 0^+} \text{Im} \mathcal{G}(\mathbf{k}, \epsilon + i\eta). \quad (5)$$

Since CPT is based on a perturbation expansion in the inter-cluster hopping, the method can be expected to work especially well in the strong-coupling regime. This is also illustrated by the fact that it becomes exact in the atomic limit, as mentioned above. On the other hand, for weak or intermediate coupling, the electronic kinetic energy is not small compared to the local interactions. Consequently, the size of the cluster has to be large enough in order to obtain accurate results. In fact, from previous applications of CPT, e.g., to the one- and two-dimensional Hubbard model,^{4,5,8} the cluster size N emerged as the main control parameter of the method. In the case of the one-dimensional Hubbard model, for example, $N = 1$ is identical to the Hubbard I approximation,²⁰ while $N = 2$ already gives a spectral function that contains most of the relevant features such as short-range antiferromagnetic ordering.⁵ With increasing N , the CPT Green function approaches systematically the exact result for the infinite system. For identical cluster size, the CPT spectrum contains many more poles with significant residues than the corresponding results of ED. In fact, also in the 1D Hubbard model, the spectrum obtained with CPT on a four-site cluster is already comparable in quality to the ED spectrum for $N = 12$ (Refs. 4,5). An additional advantage of CPT is the possibility to evaluate $A(\mathbf{k}, \epsilon)$ at continuous wavevectors \mathbf{k} , in contrast to ED which restricts \mathbf{k} to the N vectors of the first Brillouin zone of the cluster, of which only $N/2 + 1$ are physically distinct. Finally, finite temperature Lanczos methods can also be combined with CPT to calculate thermodynamic properties.⁹

Concerning the application of the Lanczos method to calculate the cluster Green function G_{ab} , it is important to stress the need for open boundary conditions (BCs). Attempts have been made to use periodic BCs and subtract the corresponding terms afterward in the perturbative treatment of the inter-cluster hopping, but it has been found that the accuracy of the results is much better for the case of open BCs. Although the latter are physically more intuitive in connection with CPT, the calculation of the cluster Green function with the Lanczos method becomes more difficult as one cannot exploit

translational symmetry. Other symmetries such as the inversion group can be used in principle, but are usually not as effective in saving computer memory by reducing the size of the corresponding Hamiltonian matrix and Lanczos vectors.

We want to point out that CPT does not in principle rely on the ED method. In fact, the cluster Green function may be calculated using any method available.⁵ Indeed we will see in Sec. IV that it is possible to combine the exact analytic solution for the atomic-limit Green function with CPT, to obtain results which agree surprisingly well with the many-body coherent potential approximation.¹⁹

In addition to the spectral function considered here, other physical properties of the system can also be calculated with CPT. This includes, e.g., the ground state energy of the infinite system, the electronic kinetic energy or the Fermi surface.⁵ The strength of CPT lies in the calculation of the one-particle Green function and related quantities such as the density of states. The numerical effort is relatively small compared to more sophisticated methods like DMRG or QMC. An additional advantage of CPT is the fact that it can easily be applied also to two-dimensional systems, in contrast to, e.g., DMRG. Finally, an important disadvantage of CPT should be mentioned: Within the current formulation, two-particle Green functions cannot be calculated. Consequently, it is not possible to compute, e.g., the dc conductivity or other interesting two-particle correlation functions.

III. HOLSTEIN POLARON

The Hamiltonian of the Holstein model¹⁵ reads

$$H = -t \sum_{\langle ij \rangle \sigma} (c_{i\sigma}^\dagger c_{j\sigma} + \text{h.c.}) + \omega \sum_i b_i^\dagger b_i - g \sum_i n_i (b_i^\dagger + b_i), \quad (6)$$

where $c_{i\sigma}^\dagger$ ($c_{i\sigma}$) and b_i^\dagger (b_i) are creation (annihilation) operators for an electron with spin σ and a phonon of frequency ω at lattice site i , respectively. The electron occupation number is defined as $n_i = \sum_\sigma n_{i\sigma}$ with $n_{i\sigma} = c_{i\sigma}^\dagger c_{i\sigma}$, and the parameters of the model are the hopping integral for nearest-neighbor hopping, t , and the electron-phonon coupling strength, denoted as g . It is common to define a dimensionless coupling parameter $\lambda = g^2/(2\omega W)$, where $2W$ is the bandwidth of the bare electron band, and a dimensionless phonon frequency $\bar{\omega} = \omega/t$. The Holstein model can then be described using only these two parameters. Moreover, we shall express all energies in units of t . As mentioned above, here we only consider the one-electron limit of Hamiltonian (6) which is also called the Holstein polaron problem. Although there is only a single electron in the system, the coupling to the phonons makes it a complex many-body problem, which has been the focus of much theoretical work. The

restriction to one electron greatly simplifies calculations with the Lanczos method since both, the number of required phonon states²¹ and the number of electron configurations grow noticeably with the number of particles. However, in Sec. IV, we will use the exact result for the atomic-limit Green function and CPT for a single-site cluster to calculate the spectral function of the Holstein model of spinless fermions at quarter-filling.

Following other authors,^{22,23,24,25,26,27} we calculate the Green function

$$\mathcal{G}(\mathbf{k}, \epsilon) = \langle 0 | c_{\mathbf{k}} \frac{1}{\epsilon - H} c_{\mathbf{k}}^\dagger | 0 \rangle, \quad (7)$$

where $|0\rangle$ represents the ground state of the phonons and the vacuum state for the electrons. The spin index can be suppressed due to the symmetry of the problem. The corresponding one-electron spectral function is given by Eq. (5).

Compared to the class of Hubbard models for which CPT has been originally developed, we are facing an additional difficulty arising from the a priori infinite number of allowed phonon states. We employ a widely used truncation scheme²³ of the phonon Hilbert space which is spanned by the basis states

$$|r\rangle_{\text{ph}} = \prod_{i=1}^N \frac{1}{\sqrt{\nu_i^{(r)}!}} (b_i^\dagger)^{\nu_i^{(r)}} |0\rangle_{\text{ph}}, \quad (8)$$

where $\nu_i^{(r)}$ denotes the number of phonons at lattice site i . Now the truncation consists in restricting the basis states to the subset with

$$\sum_{i=1}^N \nu_i^{(r)} \leq N_{\text{ph}} \quad (9)$$

leading to $(N_{\text{ph}} + N - 1)!/(N_{\text{ph}}!(N - 1)!)$ allowed phonon configurations. The convergence of the results with N_{ph} can be monitored using the ground-state energy E of the cluster with open BCs. In all results of this paper, N_{ph} was chosen such that the relative error for the ground state with one electron, $|E(N_{\text{ph}} + 1) - E(N_{\text{ph}})|/|E(N_{\text{ph}})|$, was smaller than 10^{-5} . We find that convergence of E also ensures a well-converged spectral function. Moreover, the influence of the number of phonons kept in the calculation is much larger for the incoherent part of the spectrum than for the coherent, low-energy quasi-particle peak which determines E (see Sec. III A). Finally, a refined truncation scheme which allows for extremely accurate results (relative error $< 10^{-7}$) has been proposed by Wellein et al.²⁸

Before we come to a discussion of the results obtained with CPT, we want to comment on some of the existing work on spectral properties of the Holstein polaron. As indicated before, the most reliable method to calculate dynamic quantities, such as $A(\mathbf{k}, \epsilon)$, is ED which has been used extensively in the past.^{22,23,24,25,26,27,28,29,30} Most of this work has focused on the polaron band structure $E(\mathbf{k})$

instead of the spectral function, since it is often easier to interpret, especially in the strong-coupling regime where the structure of $A(\mathbf{k}, \epsilon)$ is rather complicated. However, as pointed out by Wellein et al.,²⁸ the two quantities are closely related. In fact the position of the lowest-energy peak in $A(\mathbf{k}, \epsilon)$, obtained from the Green function (7), follows exactly the polaron band structure as we vary \mathbf{k} . Moreover, as discussed by Wellein and Fehske,²⁹ the integral over this first peak is equivalent to the quasi-particle (QP) weight $z(\mathbf{k}) = |\langle \psi_{0,\mathbf{k}}^{(1)} | c_{\mathbf{k}}^\dagger | 0 \rangle|^2$, where $\psi_{0,\mathbf{k}}^{(1)}$ denotes the lowest-energy single-polaron state in the sector with total momentum \mathbf{k} . Other numerical methods which have been used to calculate the spectrum of the Holstein polaron include DMRG^{31,32} (in one dimension), finite-cluster strong coupling perturbation theory³³ (1D, 2D), QMC^{34,35} (1D–3D), and variational methods^{36,37,38} (1D–4D).

A. Comparison with Exact Diagonalization

As mentioned above, the critical parameter of CPT is the number of sites in the cluster. To demonstrate the advantage of CPT over the standard ED method (see, e.g., Ref. 23) we present in Fig. 1 the spectral function $A(0, \epsilon)$ in one dimension for different cluster sizes N . We chose $\bar{\omega} = 2$ and $\lambda = 0.5$, which is the regime where an extended polaron exists (see, e.g., Ref. 28). Consequently, significant finite-size effects can be expected for small clusters, which is exactly what we see in the ED results. For the latter periodic BCs have been used. Fig. 1 clearly shows that the shape of the large QP peak at $\epsilon \approx -2.4$ changes very little with increasing N for both, ED and CPT, but a noticeable shift can be observed in the case of the ED spectra as we go from $N = 2$ to $N = 4$. The influence of N is much larger for the incoherent part of the spectrum, which lies about a distance $\bar{\omega}$ above the QP peak. The ED spectra display sharp, well-separated peaks, whereas the corresponding CPT data—containing many more poles—resembles much closer the expected results for an infinite system. The latter has been investigated by Marsiglio²³ using Migdal-Eliashberg theory. For the same parameters, he found that the QP peak remains almost unchanged as $N \rightarrow \infty$, while the incoherent part evolves into a continuous band that fits well to the CPT results even for rather small clusters $N \gtrsim 6$. We have also compared $A(k, \epsilon)$ for $k \neq 0$, and the observed influence of finite-size effects agrees perfectly with previous work of Wellein and Fehske.²⁹ As k increases from $k = 0$ to $k = \pi$, the size of the polaron increases, and the deviations of the ED data from the CPT results become larger. In the strong-coupling or small-polaron regime, not shown here, finite-size effects are known to be small. Consequently, even for very small clusters, ED and CPT both give well-converged results for the QP peak which determines, e.g., the ground-state energy. However, in the case of ED, the incoherent part of the spectrum for wavevector k , corresponding to excitations of an electron

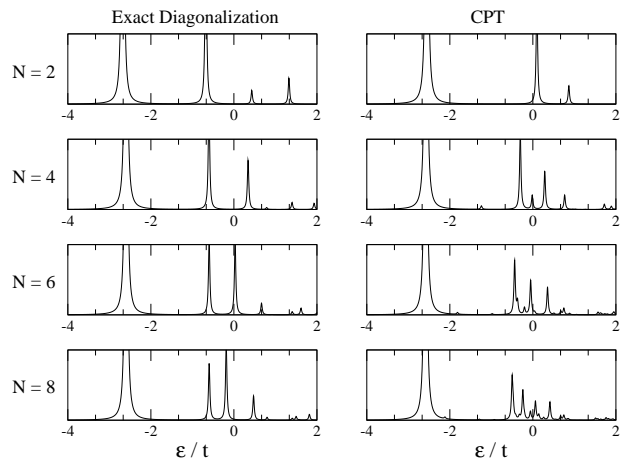


FIG. 1: Comparison of the spectral function $A(0, \epsilon)$ of the 1D Holstein polaron obtained with ED (left column) and CPT (right column) for various numbers of lattice sites N in the cluster. The plot is for $\bar{\omega} = 2.0$, $\lambda = 0.5$ and $N_{\text{ph}} = 6$. An artificial imaginary part $\eta = 0.02t$ has been used to broaden the delta peaks.

with momentum q and a phonon with momentum $k - q$, still exhibits the typical multi-peak structure of a finite system, whereas the CPT results again reproduce much better the incoherent band found in the thermodynamic limit. Moreover, as mentioned in Sec. II, CPT allows to calculate $A(k, \epsilon)$ for continuous k , while ED on a N -site cluster is restricted to $N/2 + 1$ physically non-equivalent wavevectors.

A closer look at the CPT results in Fig. 1 reveals small additional peaks—not present in the ED spectra—which move from the incoherent part of $A(k, \epsilon)$ towards the QP peak with increasing N . Additional calculations for larger clusters have shown that these peaks vanish systematically with increasing N , so that the CPT spectrum approaches the exact result in the thermodynamic limit $N = \infty$, as expected. Consequently, these peaks are not a defect of CPT, but represent finite-size effects which arise from the approximate treatment of inter-cluster hopping. The latter, in combination with the open BCs used to calculate the cluster Green function, leads to a system which does not have perfect translational symmetry. The situation is equivalent to ED with open BCs: For $N \rightarrow \infty$ the spectrum approaches the results of an infinite cluster. However, in contrast to CPT, the effects for finite N are much more significant. Moreover, these finite-size effects manifest themselves in a slightly different way than in the case of periodic BCs, where no additional peaks—showing the afore mentioned behavior—are found. In the case of CPT, already for the small cluster sizes shown in Fig. 1, the spectral weight of these additional peaks is extremely small compared to the rest of the spectrum. For other values of $\bar{\omega}$ and λ , a similar behavior has been found. Although not discussed by the authors, similar effects can also be expected for the case of the Hubbard model,^{4,5,8} although they may be larger for the Holstein polaron

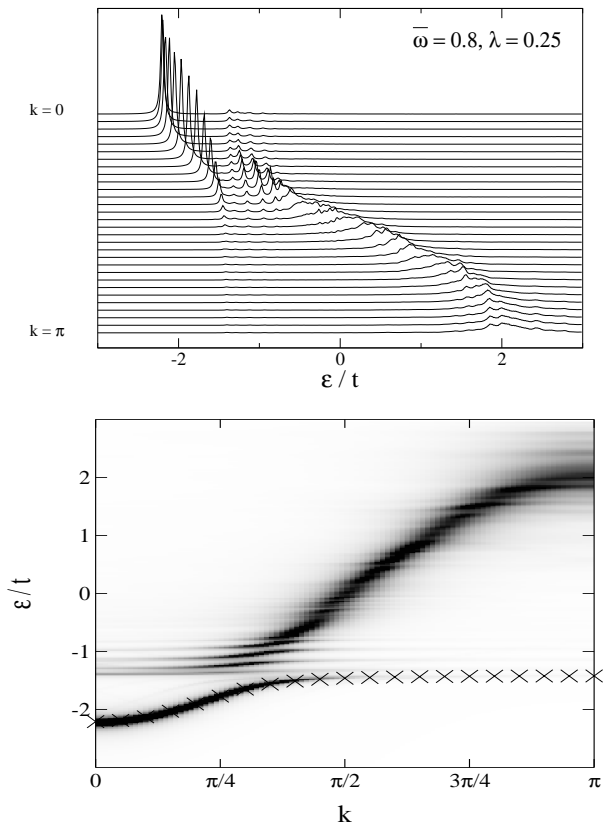


FIG. 2: Top: Spectral function $A(k, \epsilon)$ of the 1D Holstein polaron calculated with CPT for $N = 14$, $N_{\text{ph}} = 6$ and $\eta = 0.02t$. Bottom: Density plot of the same data for 100 points in k space. Symbols represent results of Bonča et al.³⁷

due to the higher sensitivity of phonon-excitations to the BCs.

B. Results: One dimension

In one dimension, the general picture emerging from previous work on the Holstein polaron problem is as follows (see e.g. Ref. 28 and references therein): In the non-adiabatic regime ($\bar{\omega} > 1$), a so-called Lang-Firsov polaron is formed which, due to the instant response of the phonons to the electronic motion, represents a very localized object. As the electron-phonon coupling increases, its mobility or effective hopping amplitude exhibits a gradual decrease, and for strong coupling a nearly-localized small polaron moving in an exponentially narrow band exists. In contrast, in the adiabatic ($\bar{\omega} < 1$), weak-coupling regime the electron drags with it an extended cloud of phonons. This object is usually called a ‘large polaron’. At $\lambda \approx 1$, a sharp but continuous³⁹ transition to a less mobile small Holstein polaron takes place. The two conditions for small-polaron formation, independent of the value of $\bar{\omega}$, are $\lambda > 1$ and $\lambda/\bar{\omega} > 0.5$.²⁸ Moreover, as pointed out by Capone et al.,⁴⁰ the formation of small polarons is determined by $\lambda > 1$ for $\bar{\omega} < 1$

and by $\lambda/\bar{\omega} > 0.5$ for $\bar{\omega} > 1$. Here we restrict ourselves to the most interesting regime of phonon energies comparable to the electronic hopping, i.e. $\bar{\omega} \sim 1$. For intermediate $\bar{\omega}$ and λ , no reliable analytical methods exist, so that numerical approaches represent the most important source of information.

In Fig. 2 we present results for $A(k, \epsilon)$ for $\bar{\omega} = 0.8$, $\lambda = 0.25$ and $N = 14$, as well as a density plot of the same data. As mentioned before, the spectrum consists of a low-lying QP peak and an incoherent part at higher energies. The physics behind the observed behavior of $A(k, \epsilon)$ has been discussed, e.g., by Stephan,³³ and is typical for electronic systems weakly interacting with dispersionless optical phonons. For small k , most of the spectral weight resides in the QP peak which corresponds to a weakly-dressed electron. For the case considered here, in which the phonon energy lies inside the bare electron band, electron and phonon hybridize and repel each other near the point where they would be degenerate, i.e. for $|E(k) - E(0)| \sim \bar{\omega}$. This coincides with the region where the flattening of the polaron band occurs and, in fact, for larger k the phonon becomes the lowest-energy excitation. However, most of the spectral weight is contained in the broad, incoherent band which follows the free-electron dispersion. The density plot in Fig. 2 also contains data for the polaron band structure $E(k)$ which has been obtained by Bonča et al.³⁷ using their variational ED method. The latter has been shown to give very accurate results for the infinite system, although it becomes somewhat less accurate in the strong coupling regime and for large values of k (Ref. 37). As mentioned before, $E(k)$ corresponds to the lowest-energy band in $A(k, \epsilon)$ and we find very good agreement with our data throughout the Brillouin zone.

Fig. 3 shows results for a similar phonon frequency $\bar{\omega} = 1.0$ but for stronger electron-phonon coupling $\lambda = 0.5$ and $N = 12$. Compared to the weak-coupling case discussed above, the polaron band is separated more clearly from the incoherent part of the spectrum and, as expected, the band-width is further reduced. Additionally, even more spectral weight has been transferred to the high-energy, incoherent band. On top of that, a gap shows up in the upper band at about $k = \pi/2$. Again the polaron band fits very well the results for $E(k)$ of Bonča et al.³⁷

We next consider the case of intermediate coupling $\lambda = 1.0$, with $\bar{\omega} = 1$ and $N = 8$ (Fig. 4). For these parameters, an extended polaron exists which still has a relatively large band-width, compared to the small-polaron case discussed below. Moreover, the incoherent part of the spectrum has split up into several sub-bands separated in energy by $\bar{\omega}$, which correspond to excitations of an electron and one or more phonons. As before, we find very good agreement between the low-energy band in $A(k, \epsilon)$ and the polaron band energy $E(k)$ calculated by Bonča.⁴¹

Finally, in Fig. 5, we report the spectral function for $\bar{\omega} = 1$ and $\lambda = 2.0$. The results have been obtained using only a four-site cluster, which is sufficient to get very

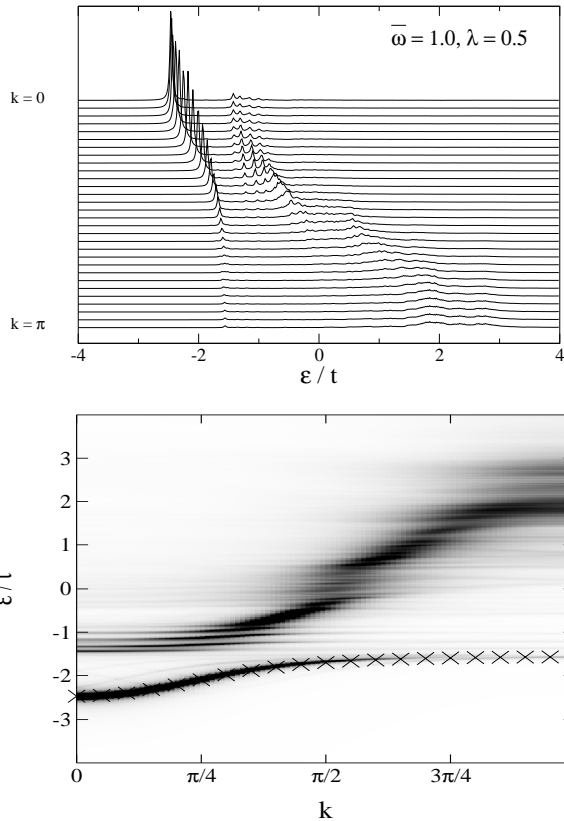


FIG. 3: Top: Spectral function $A(k, \epsilon)$ of the 1D Holstein polaron calculated with CPT for $N = 12$, $N_{\text{ph}} = 6$ and $\eta = 0.02t$. Bottom: Density plot of the same data for 100 points in k space. Symbols represent results of Bonča et al.³⁷

good agreement with Bonča’s data for $E(k)$, with only minor deviations at large values of k where finite-size effects are most pronounced, as discussed in Sec. III A. This is a consequence of the predominantly local effects in the strong-coupling regime, which also manifest themselves in terms of a very narrow polaron band.

C. Results: Two dimensions

To illustrate the applicability of CPT, we also calculated the spectral function of the Holstein polaron on a 2D cluster with $N = 8$, which has the shape of a tilted square. In contrast to CPT in one dimension, the choice for the shape of the cluster is not unique, and different clusters may lead to slightly different results. This possibility has been investigated for the Hubbard model, and the effect of the cluster shape on $A(\mathbf{k}, \epsilon)$ was found to be rather small.⁵ For the case of the Holstein polaron, where the physics is dominated by local correlations, the influence of the geometry of the cluster is expected to be even smaller.

As discussed, e.g., by Wellein et al.,²⁸ similar to 1D, a small polaron is formed in two dimensions provided that $\lambda > 1$ and $\lambda/\bar{\omega} > 0.5$. While the behavior in the

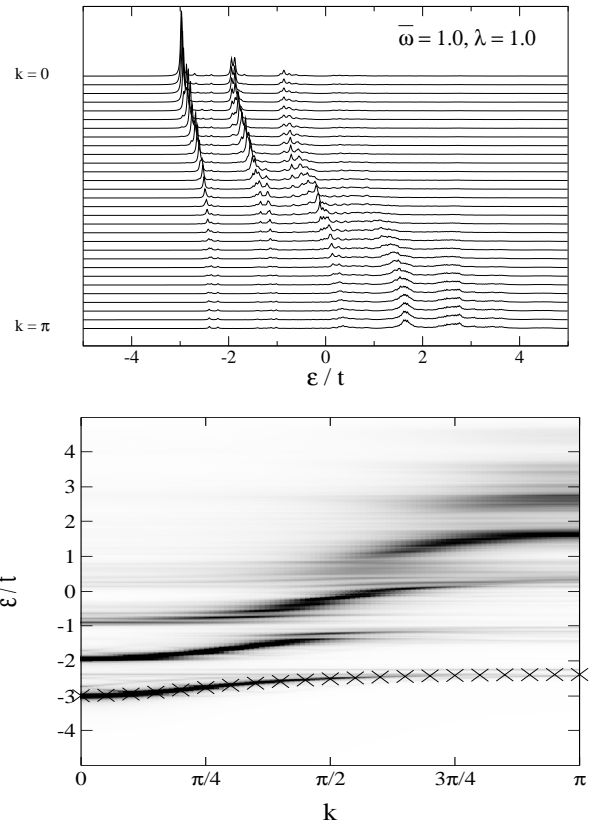


FIG. 4: Top: Spectral function $A(k, \epsilon)$ of the 1D Holstein polaron calculated with CPT for $N = 8$, $N_{\text{ph}} = 9$ and $\eta = 0.02t$. Bottom: Density plot of the same data for 100 points in k space. Symbols represent results of Bonča.⁴¹

non-adiabatic regime ($\bar{\omega} > 1$) is only weakly affected by dimensionality,^{28,42} important differences exist in the adiabatic regime $\bar{\omega} < 1$: In contrast to the one-dimensional case, where a large polaron is formed for any $\lambda > 0$, the electron remains quasi-free for $\lambda < 1$, as indicated by an almost unaffected effective hopping amplitude. Moreover, for the same value of $\bar{\omega}$, the cross-over to a small polaron at $\lambda \approx 1$ is much sharper in 2D than in 1D.

Here we simply aim to demonstrate the possibility of calculating the 2D spectral function with CPT. Therefore, we restrict ourselves to one set of parameters, namely $\bar{\omega} = 2.0$ and $\lambda = 0.945$, which has also been treated using *finite-cluster* strong-coupling perturbation theory³³. In contrast to standard SCPT based on the Lang-Firsov transformation, the latter has been shown to give reliable results also for intermediate λ and $\bar{\omega}$, which is a consequence of the inclusion of longer-ranged effects.^{29,33} While in the 1D case the density plot of $A(\mathbf{k}, \epsilon)$ contains all 100 values of k used in CPT, in two dimensions we have used 400 points in \mathbf{k} space. However only 60, lying along $\Gamma\text{MX}\Gamma$, are shown in Fig. 6.

From the above discussion, and for the parameters considered here, we expect a rather broad polaron band. This is clearly confirmed by the spectral function shown in Fig. 6, and the lowest-energy band in our data resem-

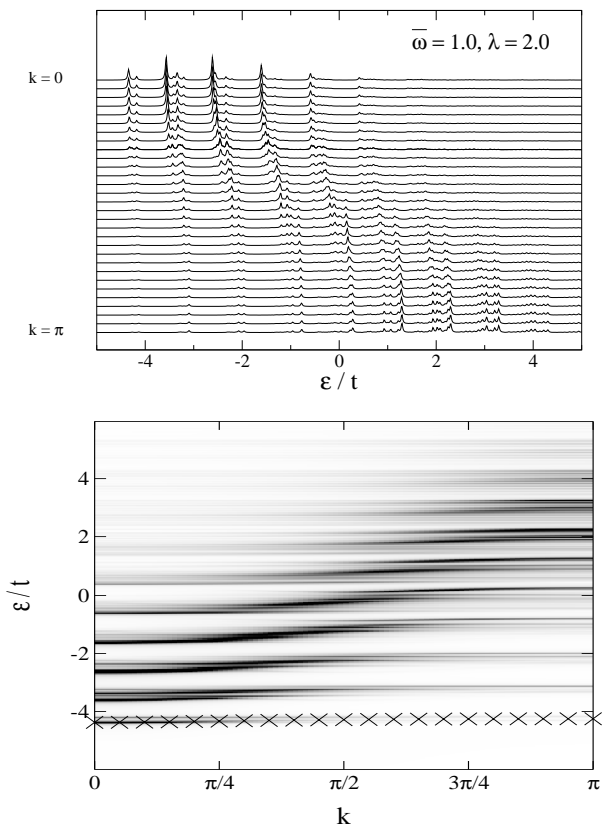


FIG. 5: Top: Spectral function $A(k, \epsilon)$ of the 1D Holstein polaron calculated with CPT for $N = 4$, $N_{\text{ph}} = 25$ and $\eta = 0.02t$. Bottom: Density plot of the same data for 100 points in k space. Symbols represent results of Bonča.⁴¹

bles closely the findings of Stephan (Fig. 2 of Ref. 33). In particular, similar to the one-dimensional case considered in Sec. III B, a flattening of the polaron band near $(\pi/2, \pi)$ is found which has also been noted by Wellein et al.²⁸ Above the polaron band, also similar to 1D, there lie several other incoherent bands which correspond to multi-phonon excitations and are therefore separated in energy by $\bar{\omega}$.

In summary, the results of this section clearly demonstrate that CPT is applicable not only in the strong-coupling regime, but also for weak and intermediate electron-phonon interaction. The quality of the resulting spectra is superior to ED data for the same cluster size, and very good agreement has been found with the variational method of Bonča et al.³⁷ in one dimension. Moreover, we have shown that CPT also allows accurate calculations of $A(\mathbf{k}, \epsilon)$ in two dimensions.

IV. MANY-ELECTRON CASE

In the last section, we have restricted ourselves to the Holstein model with one electron. Although CPT has been successfully applied, e.g., to the many-electron Hubbard model,^{4,5,8,9} the electron-phonon coupling in

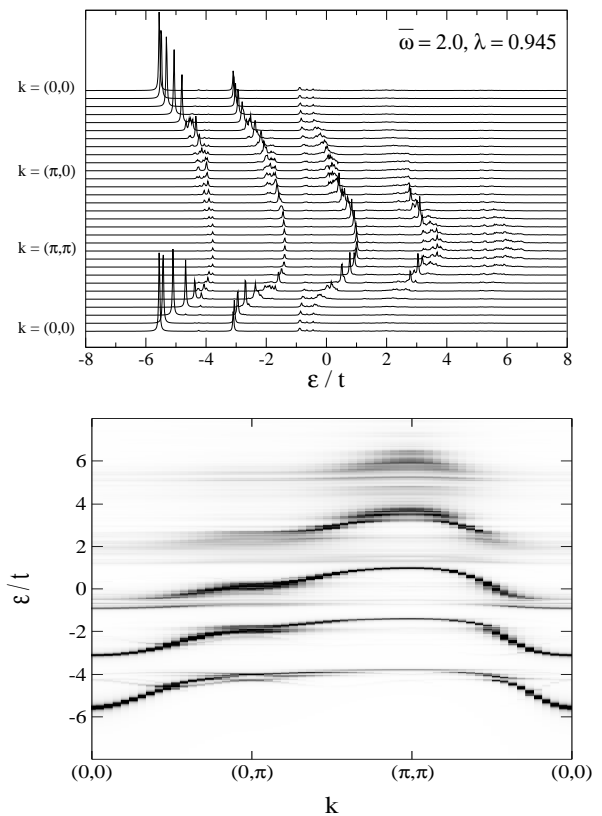


FIG. 6: Top: Spectral function $A(\mathbf{k}, \epsilon)$ of the 2D Holstein polaron calculated with CPT for $N = 8$, $N_{\text{ph}} = 9$ and $\eta = 0.02t$. Bottom: Density plot of the same data (see text).

the Holstein model greatly complicates calculations using Lanczos ED. For finite electron density, we combine CPT with the exact analytic result for the Green function in the atomic limit. For the atomic limit, the Green function has been obtained for many models using the equation-of-motion method,⁴³ and here it will allow us to obtain results for the many-electron case which will be compared with the many-body coherent potential approximation discussed below.

A. Many-body coherent potential approximation

Extending previous work of Edwards et al.^{17,18} for the pure double-exchange (DE) model (see, e.g., Ref. 14), Green¹⁶ studied the Holstein-DE model using a many-body coherent potential approximation (CPA) which, owing to the more complicated form of the Holstein-DE Hamiltonian, constitutes a considerable extension of the Hubbard III approximation.⁴⁴ The many-body CPA successfully describes many aspects of the manganites, and we refer the reader to a recent review of this work by Edwards.¹⁴ Here we only consider the special case of a completely saturated ferromagnetic state at temperature $T = 0$, with all itinerant spins having \uparrow spin, say. Consequently, the DE term which couples local and itinerant

spins¹⁴ becomes merely a constant shift in energy, and the Holstein-DE model is equivalent to the pure Holstein model of spinless fermions, i.e. with no doubly-occupied sites.¹⁹ An important feature of the many-body CPA is that the one-electron Green function reduces to the exact atomic limit for $t = 0$, which takes the form¹⁹

$$G_{\uparrow}^{\text{AL}}(\epsilon) = e^{-\alpha} \left\{ \frac{1}{\epsilon} + \sum_{r=1}^{\infty} \frac{\alpha^r}{r!} \left(\frac{n}{\epsilon + \omega r} + \frac{1-n}{\epsilon - \omega r} \right) \right\}, \quad (10)$$

where $\alpha = g^2/\omega^2$ and the polaron binding energy $-(g^2/\omega)n$ ($n = 0, 1$) has been absorbed into the chemical potential. The general result for G^{AL} of the Holstein model with electrons of both spins has been given by Green,¹⁶ and we drop the spin-index in the sequel. As discussed by Edwards,¹⁴ for an elliptic density of states, the local Green function $\mathcal{G}(z)$ for complex energy z satisfies the CPA equation

$$\mathcal{G}(z) = G^{\text{AL}}(z - W^2\mathcal{G}/4) \quad (11)$$

and the self-energy can be obtained from¹⁴

$$\Sigma(z) = z - \mathcal{G}^{-1} - W^2\mathcal{G}/4. \quad (12)$$

Finally, the one-electron spectral function is given by

$$A(\mathbf{k}, \epsilon) = -\pi^{-1} \text{Im} [z - \epsilon_{\mathbf{k}} - \Sigma(z)], \quad (13)$$

where

$$\epsilon_{\mathbf{k}} = -2t \sum_{m=1}^3 \cos k_m \quad (14)$$

is the band energy for wavevector \mathbf{k} .

In order to compare with angle-resolved photoemission (ARPES) data on the bilayer manganite $\text{La}_{1.2}\text{Sr}_{1.8}\text{Mn}_2\text{O}_7$, nominally with $n = 0.6$, Hohenadler and Edwards chose a strong-electron phonon coupling $g/W = 0.2$, as deduced from the low Curie temperature of this material.¹⁹ To simplify calculations, they also used $n = 0.5$ for which case the chemical potential $\mu = 0$ by symmetry. We want to point out that the many-body CPA assumes a homogeneous system, so that no tendencies toward charge-density-wave order occur as n is varied.¹⁶ As in previous work,¹⁶ Hohenadler and Edwards used $W = 1\text{eV}$ and $\omega/W = 0.05$ (see also Ref. 14). The results¹⁹ for $A(\mathbf{k}, \epsilon)$, shown in Fig. 7, support the theory of Alexandrov and Bratkovsky⁴⁵ that in these manganites, small polarons exist in the ferromagnetic state. A similar interpretation of the experimental data—based on standard small-polaron theory—had also been given by Dessau et al.⁴⁶ Well away from the Fermi surface, a well-defined peak exists which broadens as \mathbf{k} approaches the Fermi level E_{F} at $y = 0.5$. If y is increased further, most of the spectral weight is transferred above E_{F} . Moreover, the peaks never approach the Fermi level closely, in agreement with the experimental data. This indicates the existence of a pseudogap in the one-electron density

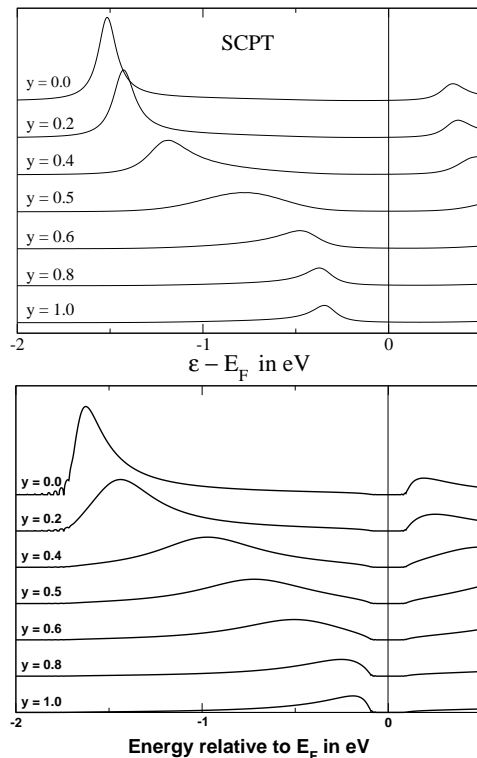


FIG. 7: Comparison of the spectral function of the Holstein model of spinless fermions at $T = 0$, calculated with SCPT (top) and with the many-body CPA (bottom, taken from Ref. 19). Here the wavevector \mathbf{k} is given by $\mathbf{k} = \pi(1, y, 0)$ with y as indicated in the figure. The plot is for $\omega/W = 0.05$ and $g/W = 0.2$. The SCPT results have been broadened using a smearing parameter $\eta/W = 0.05$.

of states. However, in the gap, there exist small polaron sub-bands (see Fig. 4 of Ref. 16) and one of them, at the Fermi level, presumably gives rise to the low but finite conductivity of the system. As discussed by Edwards,¹⁴ the many-body CPA does not give coherent states with infinite lifetime at the Fermi level, even for $T = 0$. This is typical for any CPA, and here it leads to an incoherent polaron sub-band around the Fermi level. Nevertheless, outside the central band around E_{F} , the imaginary part of the self-energy displays the correct behavior, i.e. it vanishes in the gap, between the polaron bands.

B. SCPT

In this section we use the exact result for the atomic-limit Green function of the Holstein model of spinless fermions, G^{AL} (Eq. (10)), and combine it with CPT to compare the resulting spectrum with the many-body CPA. For this case of a single-site cluster ($a \equiv b$), Eqs. (2) and (3) reduce to a single equation for the one-electron Green function⁵

$$\mathcal{G}(\mathbf{k}, z) = \frac{G^{\text{AL}}(z)}{1 - \epsilon_{\mathbf{k}} G^{\text{AL}}(z)} = \frac{1}{z - \epsilon_{\mathbf{k}} - \Sigma^{\text{AL}}(z)} \quad (15)$$

with $z = \epsilon + i\eta$ and $\epsilon_{\mathbf{k}}$ as defined by Eq. (14). Hence, as mentioned before, CPT for $N = 1$ is equivalent to the Hubbard I approximation,²⁰ but here with the more complicated atomic-limit Green function of the Holstein model given by Eq. (10). In the sequel, we shall refer to this approximation as SCPT. This is justified by the fact that the approach becomes exact for $t = 0$. Historically, a similar strong-coupling expansion for the Hubbard model^{6,7}—including higher order corrections—has been the starting point for the development of CPT.

Before we discuss the results, we would like to comment on the quality of the SCPT used here: While the many-body CPA requires a self-consistent, iterative solution of Eq. (11), the SCPT Green function is obtained from the Lehmann representation of the atomic-limit Green function (10), and the subsequent use of the resulting self-energy Σ^{AL} in Eq. (15). Similar to the original Hubbard I approximation,²⁰ the resulting Green function consists of delta peaks corresponding to states with infinite lifetime. However, due to the poles in the self-energy, there are no states at the Fermi level and the system is not a Fermi liquid. As in the many-body CPA, \mathcal{G} depends on \mathbf{k} only through the band energy $\epsilon_{\mathbf{k}}$, whereas the self-energy is local. This reliance on the atomic limit is reasonable in the strong-coupling regime considered here, where small polarons move in an extremely narrow band. Consequently, the simple perturbative treatment of the hopping term can be expected to give sensible results. Nevertheless, in SCPT, we have to use an artificial imaginary part η —which does not depend on energy—to obtain peaks of finite width. Although for large enough η there will be states at the Fermi level, the latter have only finite lifetime even for $T = 0$. Hence, both SCPT and the many-body CPA never give a Fermi liquid, but the self-consistent CPA Green function yields an imaginary part of the self-energy that shows the correct, strong energy-dependence except for the region inside the very small, incoherent polaron band around E_{F} , as discussed in Sec. IV A. Thus, as could be expected from the Hubbard I-like approximation in Eq. (15), the many-body CPA is superior to SCPT, although both approaches become exact in the atomic limit.

The spectral function obtained with SCPT using Eq. (5), also shown in Fig. 7, resembles quite closely the results of Hohenadler and Edwards.¹⁹ Although there are some differences concerning the width and the position of the peaks, the overall behavior is very similar. In particular, the broadening of the QP peak near the Fermi surface at $y = 0.5$ is well reproduced. Clearly, the success of SCPT consists in a surprisingly good agreement with the CPA data for all \mathbf{k} . Despite this agreement, CPT fails to reproduce the polaron sub-bands, and the sharp edge to the pseudogap for large values of y . Moreover, the gap is larger than in the CPA data. These shortcomings are a consequence of the rather crude approximation. Nevertheless, keeping in mind the simplicity of the ansatz, the agreement with the many-body CPA is satisfactory. We would like to point out that the SCPT

presented here can also be generalized to the Holstein-DE model with quantum spins (e.g. $S = 3/2$ appropriate for the manganites¹⁴) and at finite temperature, using the atomic-limit Green function given by Edwards.¹⁴ Finally, the approximation could be systematically improved by increasing the number of sites in the cluster, which is exactly the idea behind CPT.

However, for $N > 1$ the cluster Green function can no longer be calculated analytically and one has to resort to numerical methods such as ED as in Sec. III. Such calculations are extremely difficult for the case of quarter-filled two- or three dimensional clusters, small phonon frequency and strong electron-phonon coupling. Future work along these lines—employing optimized phonon approaches⁴⁷ (see also Sec. V)—is highly desirable in order to assess the quality of the many-body CPA results.

V. CONCLUSIONS

We have applied cluster perturbation theory to the Holstein polaron problem in one and two dimensions, and comparison with existing work has revealed very good agreement. In combination with the Lanczos method to calculate the cluster Green function, the method gives reliable results for the one-electron spectral function $A(\mathbf{k}, \epsilon)$, which become exact in the weak- and strong-coupling limit, $\lambda = 0$ and $t = 0$, respectively, and for the case of an infinite cluster. Calculations for continuous values of the wavevector \mathbf{k} are possible and, more importantly, finite-size effects are significantly reduced compared to standard ED. Our results extend previous applications of CPT to Hubbard and $t - J$ models, showing that the method is also well-suited for electron-phonon models with local interactions. As pointed out before, for more than one electron in the system, it becomes increasingly difficult to include enough phonon states so as to obtain converged results. Future work may therefore combine optimized phonon approaches⁴⁷ and CPT to investigate more complicated problems such as the many-electron case, or extended models including, e.g., a Hubbard term. The major advantage of such an approach is the possibility of using relatively small clusters while still obtaining results which are only weakly influenced by finite-size effects.

Additionally, we have used the exact atomic-limit Green function of the Holstein model of spinless fermions, to calculate the spectral function for the case quarter-filling and strong electron-phonon coupling. The results of this approximation at the Hubbard I level agree surprisingly well with the many-body CPA.

Acknowledgments

M.H. and M.A. were supported by DOC [Doctoral Scholarship Program of the Austrian Academy of Sciences]. We are grateful to Janez Bonča for providing

us with previously unpublished data, and we acknowledge helpful discussions with David Sénéchal and Maria

Daghofer. Finally, we would like to thank David M. Edwards for making valuable comments on the manuscript.

-
- * Electronic address: hohenadler@itp.tu-graz.ac.at
- ¹ O. Gunnarsson, V. Meden, and K. Schönhammer, Phys. Rev. B **50**, 10462 (1994).
 - ² V. Meden, K. Schönhammer, and O. Gunnarsson, Phys. Rev. B **50**, 11 179 (1994).
 - ³ E. Lieb and F. Y. Wu, Phys. Rev. Lett. **20**, 1445 (1968).
 - ⁴ D. Sénéchal, D. Pérez, and M. Pioro-Ladrière, Phys. Rev. Lett. **84**, 522 (2000).
 - ⁵ D. Sénéchal, D. Pérez, and D. Plouffe, Phys. Rev. B **66**, 075129 (2002).
 - ⁶ S. Pairault, D. Sénéchal, and A.-M. S. Tremblay, Phys. Rev. Lett. **80**, 5389 (1998).
 - ⁷ S. Pairault, D. Sénéchal, and A.-M. S. Tremblay, Eur. Phys. J. B **16**, 85 (2000).
 - ⁸ C. Dahnken, E. Arrigoni, and W. Hanke, J. Low. Temp. Phys. **126**, 949 (2002).
 - ⁹ M. Aichhorn, M. Daghofer, H. G. Evertz, and W. von der Linden, Phys. Rev. B **67**, 161103(R) (2003).
 - ¹⁰ M. G. Zacher, R. Eder, E. Arrigoni, and W. Hanke, Phys. Rev. Lett. **85**, 2585 (2000).
 - ¹¹ M. G. Zacher, R. Eder, E. Arrigoni, and W. Hanke, Phys. Rev. B **65**, 045109 (2002).
 - ¹² E. Dagotto, Rev. Mod. Phys. **66**, 763 (1994).
 - ¹³ Y. Bar-Yam, J. Mustre de Leon, and A. R. Bishop, eds., *Lattice Effects in High Temperature Superconductors* (World Scientific, Singapore, 1992).
 - ¹⁴ D. M. Edwards, Advances in Physics **51**, 1259 (2002).
 - ¹⁵ T. Holstein, Ann. Phys. (N.Y.) **8**, 325; **8**, 343 (1959).
 - ¹⁶ A. C. M. Green, Phys. Rev. B **63**, 205110 (2001).
 - ¹⁷ D. M. Edwards, A. C. M. Green, and K. Kubo, J. Phys.: Condens. Matter **11**, 2791 (1999).
 - ¹⁸ A. C. M. Green and D. M. Edwards, J. Phys.: Condens. Matter **11**, 10511 (1999), *erratum*, 2000, 12, 9107.
 - ¹⁹ M. Hohenadler and D. M. Edwards, J. Phys.: Condens. Matter **14**, 2547 (2002).
 - ²⁰ J. Hubbard, Proc. Roy. Soc. **276**, 238 (1963).
 - ²¹ F. Marsiglio, Physica C **244**, 21 (1995).
 - ²² J. Ranninger and U. Thibblin, Phys. Rev. B **45**, 7730 (1992).
 - ²³ F. Marsiglio, Physics Letters A **180**, 280 (1993).
 - ²⁴ A. S. Alexandrov, V. V. Kabanov, and D. K. Ray, Phys. Rev. B **49**, 9915 (1994).
 - ²⁵ H. Fehske, J. Loos, and G. Wellein, Z. Phys. B **104**, 619 (1997).
 - ²⁶ J. M. Robin, Phys. Rev. B **56**, 13 634 (1997).
 - ²⁷ E. V. L. de Mello and J. Ranninger, Phys. Rev. B **55**, 14 872 (1997).
 - ²⁸ G. Wellein, H. Roder, and H. Fehske, Phys. Rev. B **53**, 9666 (1996).
 - ²⁹ G. Wellein and H. Fehske, Phys. Rev. B **56**, 4513 (1997).
 - ³⁰ H. Fehske, J. Loos, and G. Wellein, Phys. Rev. B **61**, 8016 (2000).
 - ³¹ E. Jeckelmann and S. R. White, Phys. Rev. B **57**, 6376 (1998).
 - ³² C. Zhang, E. Jeckelmann, and S. R. White, Phys. Rev. B **60**, 14 092 (1999).
 - ³³ W. Stephan, Phys. Rev. B **54**, 8981 (1996).
 - ³⁴ P. E. Kornilovitch, Phys. Rev. Lett. **81**, 5382 (1998).
 - ³⁵ P. E. Kornilovitch, Phys. Rev. B **60**, 3237 (1999).
 - ³⁶ A. H. Romero, D. W. Brown, and K. Lindenberg, Phys. Rev. B **59**, 13728 (1999).
 - ³⁷ J. Bonča, S. A. Trugman, and I. Batistic, Phys. Rev. B **60**, 1633 (1999).
 - ³⁸ L. C. Ku, S. A. Trugman, and J. Bonča, Phys. Rev. B **65**, 174306 (2002).
 - ³⁹ H. Lowen, Phys. Rev. B **37**, 8661 (1988).
 - ⁴⁰ M. Capone, W. Stephan, and M. Grilli, Phys. Rev. B **56**, 4484 (1997).
 - ⁴¹ J. Bonča, private communication.
 - ⁴² M. Capone, S. Ciuchi, and C. Grimaldi, Europhys. Lett. **42**, 523 (1998).
 - ⁴³ G. D. Mahan, *Many-particle Physics* (Plenum Press, 1990), 2nd ed.
 - ⁴⁴ J. Hubbard, Proc. Roy. Soc. **281**, 401 (1964).
 - ⁴⁵ A. S. Alexandrov and A. M. Bratkovsky, J. Phys.: Condens. Matter **11**, L531 (1999).
 - ⁴⁶ D. S. Dessau, T. Saitoh, C.-H. Park, Z.-X. Shen, P. Villeda, N. Hamada, Y. Moritomo, and Y. Tokura, Phys. Rev. Lett. **81**, 192 (1998).
 - ⁴⁷ A. Weiße, H. Fehske, G. Wellein, and A. R. Bishop, Phys. Rev. B **62**, R747 (2000).